DESY 96-007
January 1996

Standard Model Higgs Search in the Reactions $e^+e^- \to b\bar{b} + 2$ Fermions at LEPII and NLC Energies

E. Boos

Deutsches Elektronen-Synchrotron DESY
Institut für Hochenergiephysik IfH, Zeuthen

and

Nuclear Physics Institute, Moscow State University, Russia

M. Sachwitz, H. J. Schreiber

Deutsches Elektronen-Synchrotron DESY
Institut für Hochenergiephysik IfH, Zeuthen

S. Shichanin

Deutsches Elektronen-Synchrotron DESY
Institut für Hochenergiephysik IfH, Zeuthen

and

Institute for High Energy Physics, Protvino, Moscow Region, Russia

ISSN 0418-9833

DESY 96-007 ISSN 0418-9833

January 1996

Standard Model Higgs Search in the Reactions $e^+e^- \to b\bar{b}$ + 2 fermions at LEPII and NLC Energies *

E. Boos[1,2], M. Sachwitz[1], H. J. Schreiber[1] and S. Shichanin[1,3]

[1]DESY-Institut für Hochenergiephysik, Zeuthen, FRG
[2]Nuclear Physics Institute, Moscow State University, 119899, Moscow, Russia
[3]Institute for High Energy Physics, 142284, Protvino, Moscow Region, Russia

---

* Talk given by E.B. at the Workshop on Physics and Experiments with Linear Colliders, Morioka-Appi, Japan, September 8-12 1995.

Abstract

A brief review of a complete tree-level Standard Model calculation of the reactions $e^+e^- \to b\bar{b} + 2$ fermions in the energy range of LEPII and the Next e^+e^- Linear Collider is presented. Cross sections of the Higgs boson, the total background and important subsets of background are shown as a function of the center-of-mass energy. Properties of the Higgs signal and its extraction from background are discussed.

1 Introduction

One of the most important problems in today's elementary particle physics is the understanding of the origin of the masses of the particles. In the Standard Model (SM) the fundamental particles receive masses through the interaction with a scalar field [1] which corresponds to a real physical neutral scalar particle, the Higgs boson H^0. The Higgs mass is however not predicted by the SM and experiments which have searched for it set a lower limit of $M_H \simeq 64.5$ GeV, see e.g. ref. [2]. It is expected that the main production mechanisms for the Higgs are the Higgsstrahlung off the Z boson [3], $e^+e^- \to H^0Z$, with $Z \to l\bar{l}$ $(l = e, \mu, \tau, \nu_e, \nu_\mu, \nu_\tau)$ or $Z \to q\bar{q}$ $(q = u, d, s, c, b)$ and the fusion process [4], $e^+e^- \to H^0\ l\bar{l}$ $(l = e, \nu_e)$.

If the mass of the Higgs boson is $\lesssim$140 GeV, the SM predicts its decay to be into b and $\bar{b}$ quarks, $H^0 \to b\bar{b}$, in about 85% of the cases. Thus a very promising reaction for its detection and the study of its properties is $e^+e^- \to b\bar{b}+ 2$ fermions [5].

In several studies of this reaction at LEPII and NLC energies some questions have remained unanswered. In particular, questions like: - how large are contributions from non-leading diagrams - to what extent are interferences important which might influence the Higgs signal and its properties - is it important to use a complete 4-body kinematics and a correct spin structure of matrix elements - in what cases it is neccessary to keep non-zero fermion masses were not addressed. That is why several complete tree level calculations and analyses have been carried out by our collaboration.

The reaction $e^+e^- \to b\bar{b}\,\mu^+\mu^-$ has been calculated in [6, 7, 8]. It turned out that this reaction has the cleanest signature for the Higgs but the event rate is rather small. Six times more Higgs events are expected in the reaction $e^+e^- \to b\bar{b}\nu\bar{\nu}$, to which some extra contribution comes from the fusion process $e^+e^- \longrightarrow H^0\ l\bar{l}$ $(l = e, \nu_e)$ at energies above LEPII. Complete tree level calculations of this reaction have been performed in [9, 10].

The reaction $e^+e^- \to b\bar{b}e^+e^-$ turned out to be the most complicated one from the calculational point of view, and the extraction of the Higgs signal out of a background two orders of magnitude larger requires well designed cuts [11].

Higgs production and detection potential have also been considered in the reaction $e^+e^- \to b\bar{b}+$ 2 jets [12, 8, 13]. The rate for this reaction is given by the sum of the rates for $e^+e^- \to b\bar{b}\,q\bar{q}$, where the symbol q denotes the sum over the u, d, s, c and b quark states, and $e^+e^- \to b\bar{b}$ + 2 gluons.

In this short review we follow papers [7, 9, 11, 13]. In sect. 2 we present a complete set of Standard Model diagrams for one of the reactions mentioned above and describe the method of calculation and the input parameters. We show the total cross section behaviour for all cases. In sect. 3 different background contributions and their relative weights are discussed for the most complicated case $e^+e^- \to e^+e^- b\bar{b}$. Sect. 4 is devoted to some properties of the Higgs signal and to its extraction out of the $b\bar{b}$ + 2 fermions background. Sect. 5 contains the summary and conclusions.

2 Rate of the reactions $e^+e^- \to b\bar{b}+$ 2 fermions

The calculation procedure consists of the following main steps. The generation of Feynman diagrams, the analytical expressions for the matrix elements squared and the corresponding optimized Fortran codes have been obtained by means of the computer package CompHEP [14]. The integration over phase space and the generation of the event flow have been done with the help of the adaptive Monte Carlo package BASES/SPRING [15]. One has to point out that because of the complicated phase space structure of the 4-fermion final states and the occurrence of singularities, a reasonable choice of variables and smoothing of singularities were mandatory. Today's version of CompHEP offers all the features needed to overcome these problems [14].

Our calculations include Breit-Wigner propagators for the Higgs and Z bosons, the tree-level Higgs width and the following set of parameters: $M_e = 0.0005$ GeV, $M_Z = 91.16$ GeV, $\Gamma_Z = 2.53$ GeV, $\alpha = 1/128$, $\alpha_s = 0.115$, $\sin^2\Theta_W = 0.226$, $M_W = M_Z \cos\Theta_W$, $m_b = 5$ GeV, $m_c = 1.35$ GeV, $m_s = 0.130$ GeV, $m_u = m_d = 0$ and $V_{cb} = 0.044$. The t'Hooft-Feynman gauge is used. Unphysical ghosts and Goldstone contributions, which appear as an internal property in this gauge, are included in the calculations.

For all reactions $e^+e^- \to b\bar{b}+$ 2 fermions the lowest order diagrams contain the contributions of the Higgs signal as well as different backgrounds. The general structure of the diagrams is similar in all cases. However, in the case of the most complicated reaction, $e^+e^- \to e^+e^- b\bar{b}$, there are specific contributions due

to the radiation off a neutral boson (photon or Z) from the initial electron or positron. As an example we present in Fig. 1 all possible diagrams contributing to the reaction $e^+e^- \to e^+e^- \, b\bar{b}$.

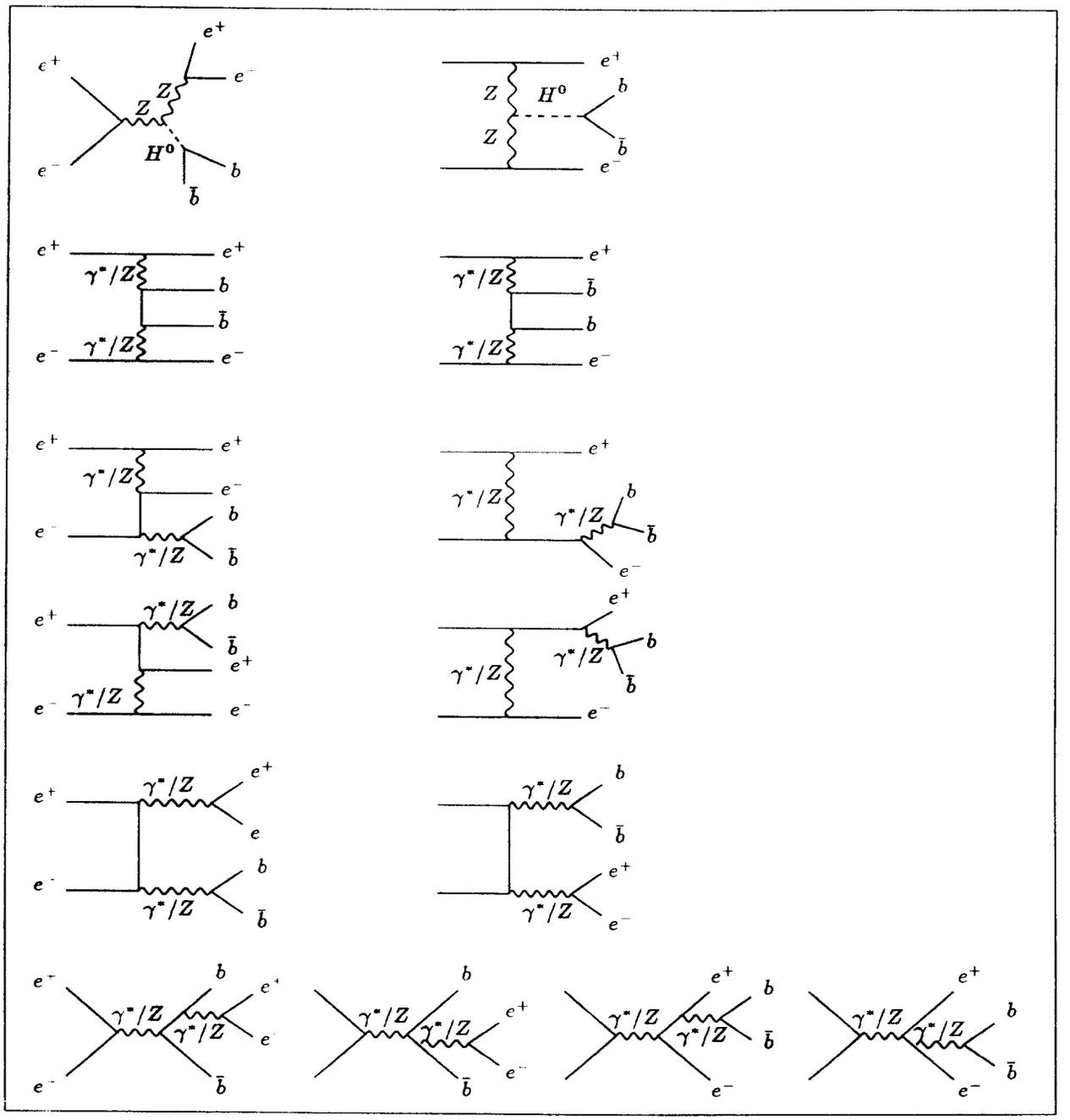

Figure 1: Feynman diagrams for the reaction $e^+e^- \to e^+e^- \, b\bar{b}$.

The two diagrams in the first row are responsible for the Higgs production either via the Higgsstrahlung process $e^+e^- \to H^0Z$ or the ZZ fusion reaction $e^+e^- \to e^+e^-H^0$. The Higgsstrahlung diagram is analogous to that in the reaction $e^+e^- \to \mu^+\mu^- \, b\bar{b}$ (or $e^+e^- \to \nu\bar{\nu} \, b\bar{b}$) with relative weights determined by the $Z \to e^+e^-$, $\mu^+\mu^-$ and $\nu\bar{\nu}$ branching fractions. The ZZ fusion contribution is

suppressed by one order of magnitude with respect to the corresponding W^+W^- fusion process in $e^+e^- \to \nu\nu\, H^0$ due to the different couplings of the Z and W boson to leptons The diagrams in the second raw are of multiperipheral nature and are governed by the 2-to-2 processes $\gamma^*(\mathrm{Z})\gamma^*(\mathrm{Z}) \to b\bar{b}$. Diagrams in the third and fourth row can be considered as due to $\gamma^*(\mathrm{Z})e^\pm \to \gamma^*(\mathrm{Z})e^\pm$ subprocesses which proceed either via electron (positron) t-channel exchanges or via s-channel processes with subsequent radiation of a $\gamma^*(\mathrm{Z})$ from an off-shell electron (positron). The fifth row of diagrams corresponds to the 2-to-2 subprocesses $e^+e^- \to \gamma^*(Z)\gamma^*(Z)$ with subsequent decays of $\gamma^*(Z)$ to e^+e^- and $b\bar{b}$. The diagrams in the last row correspond to γ^*/Z s-channel formation with $b\bar{b}$ (or e^+e^-) production and subsequent radiation of a photon/Z and its decay into e^+e^- (or $b\bar{b}$).

For the case of $q\bar{q}$ pair production in the reaction $e^+e^- \to b\bar{b} + 2$ jets there exists also a contribution when a gluon radiates off the quark and splits into a $b\bar{b}$ or $q\bar{q}$ pair.

An important step of our calculation is to split all diagrams into several subsets as indicated in Fig.1. In principle it is possible to calculate all diagrams contributing to a given reaction at once, but such calculations are technically very complicated and, in addition, the understanding of individual subsets of diagrams is lost. The last point turned out to be of importance if physical properties of subchannels are of interest. Practically, the division of the contributing diagrams into subsets is based on the occurrence of different types of singularities: s-channel resonances, t-channel bosons exchanges and s-channel photon or gluon splitting into a pair of light fermions. In addition, each subset considered is to a good approximation gauge invariant, because it is based on gauge invariant 2-to-2 and 2-to-3 subreactions. In general, the calculations show that interferences between diagrams of a particular subset are important and, due to gauge invariance, huge cancellations occur. In contrast, interferences between different subsets were found to be very small and often negligible.

The cross section for the reaction $e^+e^- \to \mu^+\mu^- b\bar{b}$ is presented in Fig. 2 as a function of the cms energy $\sqrt{s}$ for different values of the Higgs mass. One notices the typical threshold behaviour: a fast rise and a 1/s fall-off at large energies. In addition, a two-peak structure appears if the Higgs mass is ~120 GeV or larger which is due to the onset of the dominant 2-to-2 body reactions $e^+e^- \to ZZ$ and $e^+e^- \to H^0Z$ at different thresholds. For $M_H < 120$ GeV, both thresholds are close to each other and no distinct two-bump structure appears. It is interesting to note the size of the $\mu^+\mu^- b\bar{b}$ cross section itself near threshold for H^0 masses $\leq$ 100 GeV: at $\sqrt{s} = 200$ GeV, i.e. at LEPII, the 4-body final state cross section is about 50% larger if an H^0 with $M_H = 100$ GeV exists than

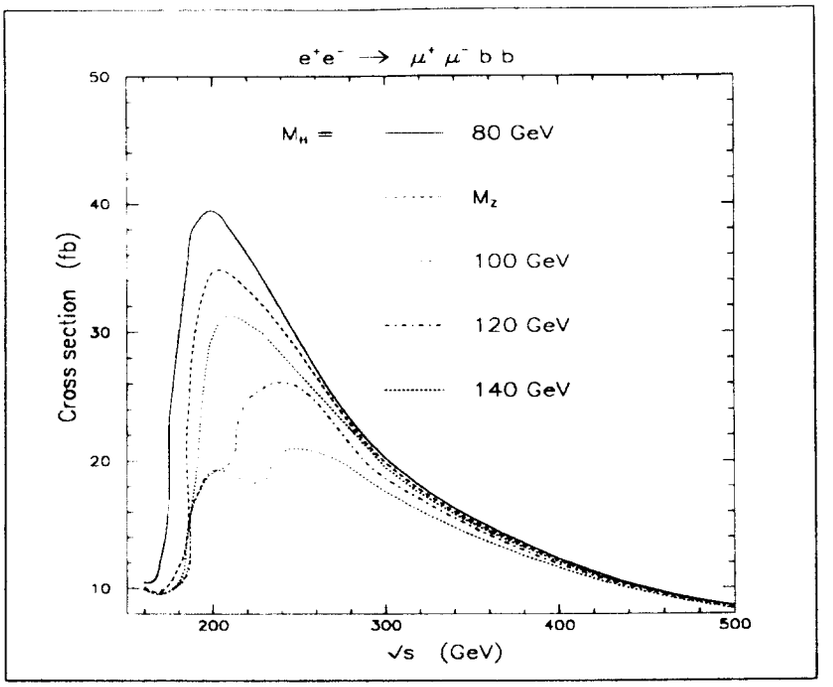

Figure 2: Cross sections of the reaction $e^+e^- \to \mu^+\mu^- b\bar{b}$ as functions of the cms energy.

without a Higgs, and twice as large for $M_H = 80$ GeV. Hence, just counting the events of $e^+e^- \to \mu^+\mu^- b\bar{b}$ provides a first hint for the existence of the Higgs boson.

Fig.3a shows the cross section for $e^+e^- \to \nu\bar{\nu}\, b\bar{b}$ as a function of the cms energy $\sqrt{s}$ at different values of the Higgs mass. The cross sections for the subreactions $e^+e^- \to (\nu_\mu\bar{\nu}_\mu + \nu_\tau\bar{\nu}_\tau)b\bar{b}$ and $e^+e^- \to \nu_e\bar{\nu}_e b\bar{b}$ are shown in Fig. 3b and c, respectively. In the energy range of LEPII their behaviour is quite similar to the $\mu^+\mu^- b\bar{b}$ case. The rise of the total $\nu\bar{\nu}\, b\bar{b}$ cross section at large energies comes from the fusion contributions of the Higgs in $e^+e^- \to \nu_e\bar{\nu}_e b\bar{b}$ as well as from $e^+e^- \to \nu_e\bar{\nu}_e Z$, with subsequent $Z \to b\bar{b}$ decay.

In Fig. 4 the total cross section for the reaction $e^+e^- \to e^+e^- b\bar{b}$ is presented as a function of $\sqrt{s}$ between 0.2 TeV and 1 TeV. In general, this behaviour is completely different from previous cases due to the dominance of the multiperipheral contributions. The cross section $\sigma(e^+e^- \to b\bar{b}\, e^+e^-)$ does not strongly vary with $\sqrt{s}$; it increases by a factor of ~ 4 in the energy range considered. In addition, Fig. 4 also shows the H^0 rate to the $e^+e^- b\bar{b}$ final state. This rate is however about two orders of magnitude lower, so that the overwhelming background has to be removed by efficient cuts without affecting the H^0 event rate expected. More details are given in sect. 4.

In Fig. 5 the total cross section for the reaction $e^+e^- \to b\bar{b}$ + 2 jets is presented as a function of $\sqrt{s}$ between 160 and 500 GeV (full curve). We

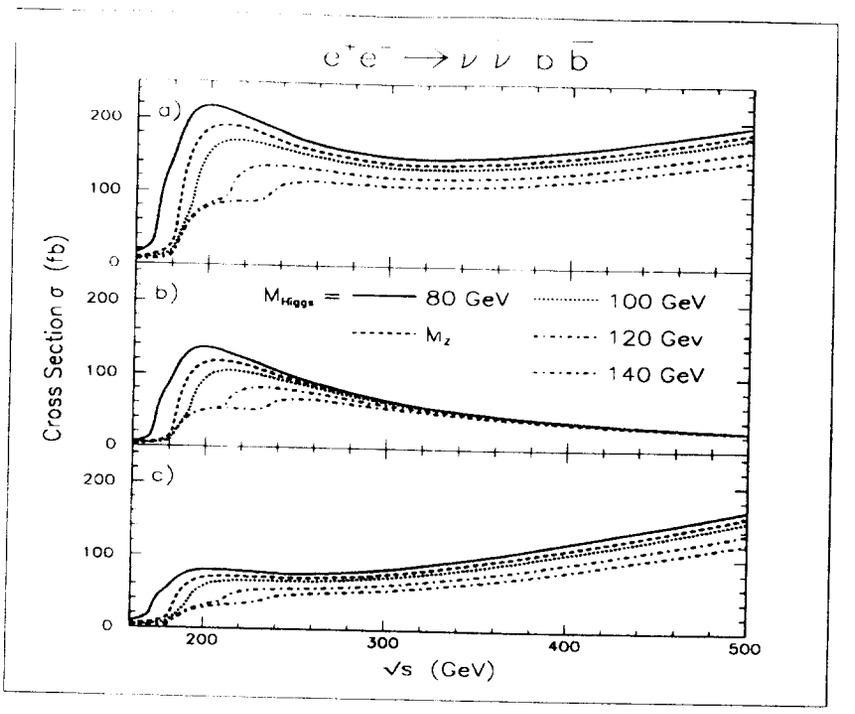

Figure 3: Cross sections of the reaction $e^+e^- \to \nu\bar{\nu}\, b\bar{b}$ as functions of the cms energy.

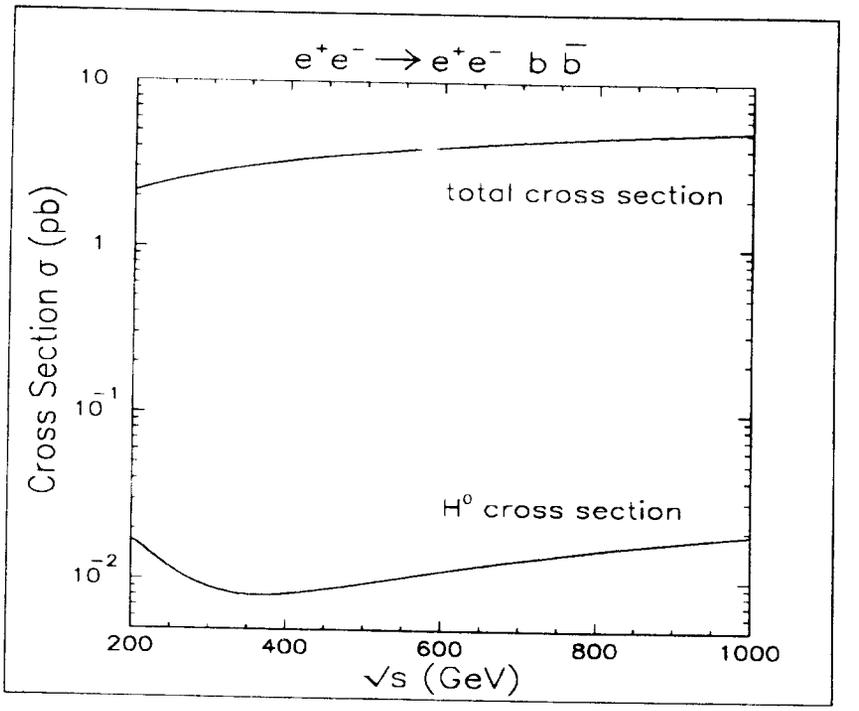

Figure 4: Cross sections of the reaction $e^+e^- \to e^+e^-\, b\bar{b}$ as functions of the cms energy.

also show in this figure the cross sections for the Higgs (with $M_H = 80$ GeV) and the background reaction $e^+e^- \to e^+e^-\, q\,\bar{q}$ as well as the cross sections for $e^+e^- \to b\bar{b} + 2$ gluons. As can be seen, the total event rate close to $\sqrt{s}$= 160 GeV

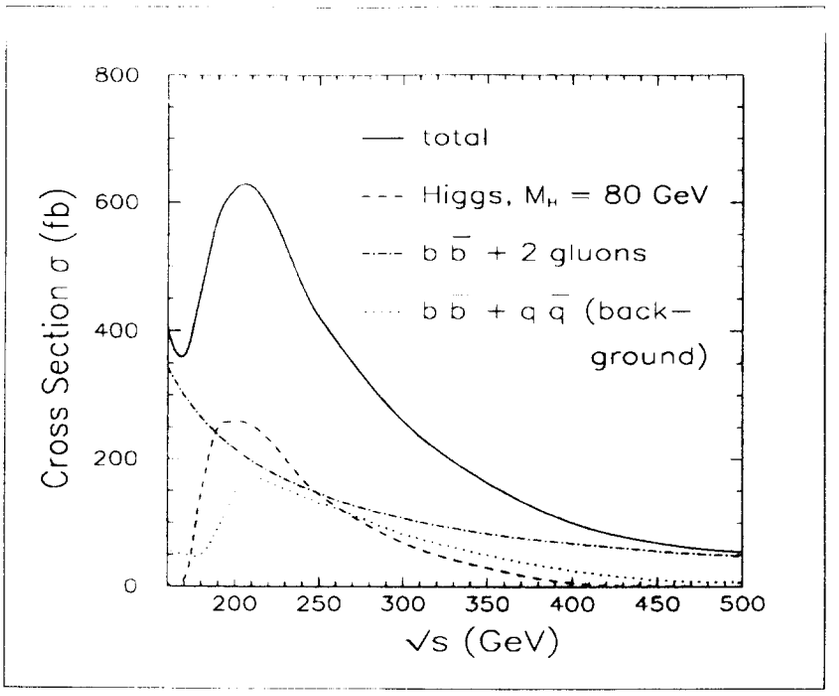

Figure 5: Cross section of the reaction $e^+e^- \to b\bar{b} + 2$ jets as functions of the cms energy.

is dominated by the 2-gluon final state which decreases as $1/s$ with increasing energy and is found to be the most important contribution above $\sqrt{s} \sim 300$ GeV. The $b\bar{b} + q\bar{q}$ background does not exceed 15% of the total rate at $\sqrt{s} \leq 170$ GeV. The sharp rise of the overall reaction cross section $e^+e^- \to b\bar{b} + 2$ jets between $\sqrt{s} \approx 170$ GeV and 200 GeV is due to the onset of the Higgs production (dashed curve) and the two-body reaction $e^+e^- \to ZZ$, with the subsequent decays of $Z \to b\bar{b}$ and $Z \to q\bar{q}$. The latter dominates the total $b\bar{b} + q\bar{q}$ background rate.

3 More details about the reaction $e^+e^- \to e^+e^- b\bar{b}$

Since the background in $e^+e^- \to e^+e^- b\bar{b}$ is about two orders of magnitude larger than the Higgs signal, it is important to investigate the possible mechanisms contributing to different phase space regions so that reasonable cuts can be applied for their suppression while retaining the H^0 signal. According to the diagram classification of Fig. 1 we present in Fig. 6 their individual contributions.

Most of the cross section for the reaction $e^+e^- \to e^+e^- b\bar{b}$ comes from the two-photon multiperipheral diagrams (second row in Fig. 1). Next important are contributions from single cascade diagrams (third and forth row in Fig. 1) with off-shell Z production and subsequent $Z \to b\bar{b}$ decay. Much less important are 2-to-2 body reactions like $e^+e^- \to \gamma^* Z$, from which that with the subsequent decays $\gamma^* \to e^+e^-$ and $Z \to b\bar{b}$ is found to be the dominant one. Double Z

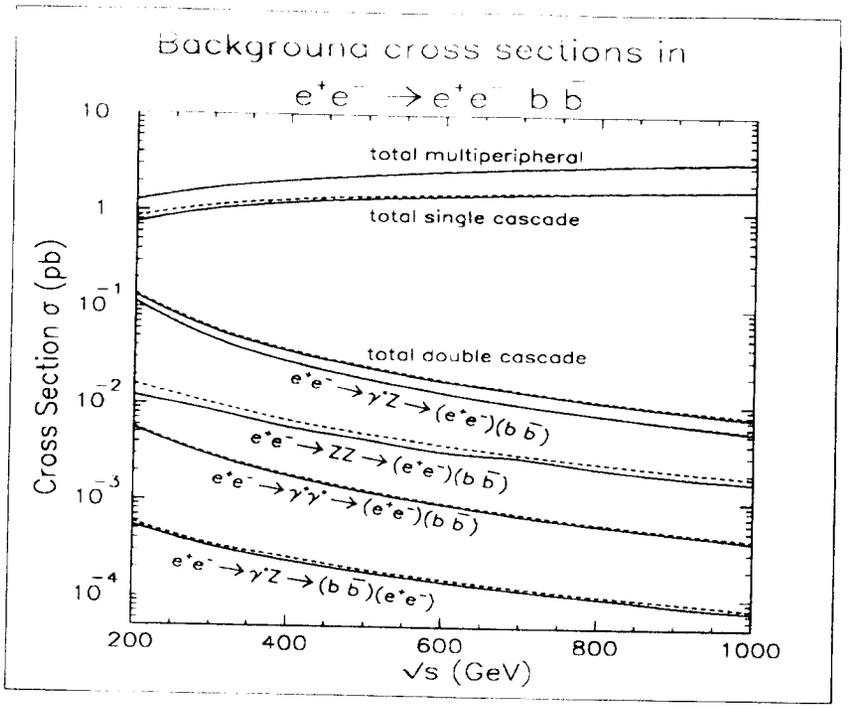

Figure 6: Cross sections for different backround reactions to the final state $e^+e^- b\bar{b}$ as function of the cms energy.

production is comparable to the Higgs production rate. Contributions due to the s-channel diagrams (last row in Fig. 1) are very small and can be neglected in the energy range studied. We have searched for significant interferences between the diagrams contributing. They were found to be negligible (smaller than 1 fb in magnitude) except the interference between single cascade diagrams with $Z \to b\bar{b}$ and double cascade diagrams with $\gamma^* \to e^+e^-$ and $Z \to b\bar{b}$ decays, and between single cascade diagrams with $\gamma^* \to e^+e^-$ and $Z \to b\bar{b}$ themselve. The dashed curves in Fig. 6 represents semianalytical calculations.

4 The extraction of the H^0 signal

Extractions of the Higgs signal from background in an efficient way have been presented in [7, 9, 11, 13]. Here we only emphasize a few points.

The reaction $e^+e^- \to e^+e^- b\bar{b}$ is interesting for at least two reasons: i) the H^0 signal is expected to be about two orders of magnitude smaller than the background and ii) large background is expected in the channel $e^+e^- \to \nu\bar{\nu}\, b\bar{b}$, from reactions with final state electrons which are missed in the detector.

Fig. 7a (8a) shows the $b\bar{b}$ invariant mass distributions for all events of the reaction $e^+e^- \to e^+e^- b\bar{b}$ expected at $\sqrt{s} = 200$ GeV ($\sqrt{s} = 500$ GeV) for an integrated luminosity of $\mathcal{L} = 500$ pb^{-1} ($\mathcal{L} = 10$ fb^{-1}). Most of the events are

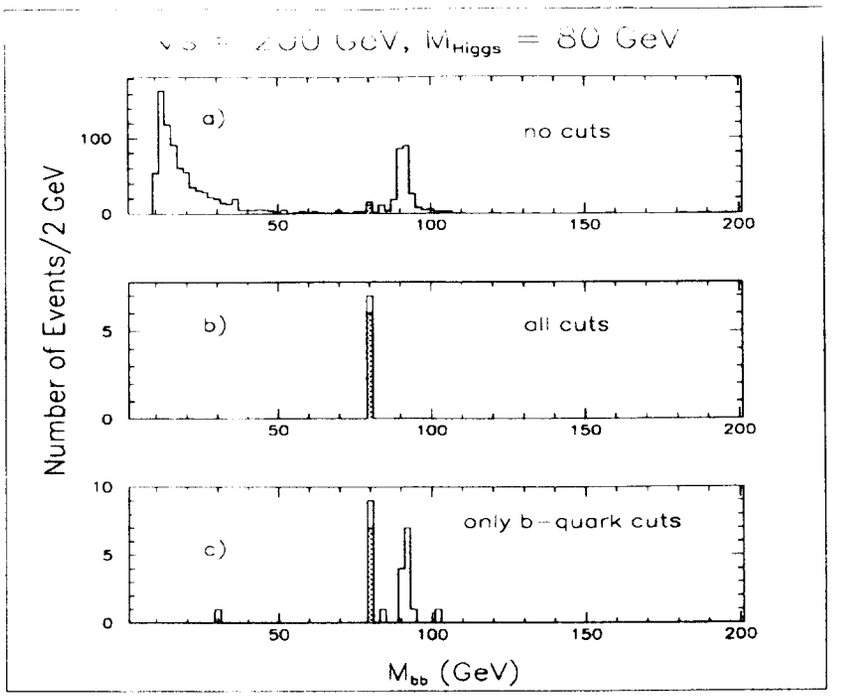

Figure 7: Number of events of the reaction $e^+e^- \to e^+e^-\, b\bar{b}$ as function of the $b\bar{b}$ invariant mass at 200 GeV for an integrated luminosity of 500 pb^{-1}.

concentrated between the $b\bar{b}$-threshold and $M_{b\bar{b}} \cong 40$ GeV, independent of $\sqrt{s}$. At 200 GeV, the Higgs boson with $M_{H^0} = 80$ GeV (shown shaded) is to a great extent hidden by the Z boson tail and additional continuum background. At 500 GeV, there exists some indication of the H^0 around 140 GeV. However, in both cases the Higgs signal is very weak in comparison with the large background. Since in most of the final states the e^- and e^+ remain undetected within the beam pipe, only cuts based on the b and $\bar{b}$ quark information are applied. Detailed studies of the signal and background distributions led to the following selection criteria:

$$|\cos\Theta_b| < 0.94, \quad |\cos\Theta_{\bar{b}}| < 0.94, \quad p_\perp^{b\bar{b}} > 45 \text{ GeV}, \quad E_{b\bar{b}} > 90 \text{ GeV} \quad \text{at 200 GeV}$$
$$|\cos\Theta_b| < 0.94, \quad |\cos\Theta_{\bar{b}}| < 0.94, \quad p_\perp^{b\bar{b}} > 10 \text{ GeV}, \quad E_{b\bar{b}} > 120 \text{ GeV} \quad \text{at 500 GeV}.$$

The resulting $M_{b\bar{b}}$ distributions are presented in Figs. 7c and 8c. Clear H^0 signals remain in both cases. Thus, the application of a few simple cuts based on b and $\bar{b}$ quark measurements allows us to extract the Higgs boson almost free of background (provided $M_{H^0} \neq M_{Z^0}$).

If one compares the $b\bar{b}$ invariant mass distributions with those of the reaction $e^+e^- \to \nu\bar{\nu}\, b\bar{b}$ (Fig.9), clear peaks from the Z and H^0 bosons are visible. A comparison with Figs. 7c and 8c indicates that there are no problems to extract the Higgs signal.

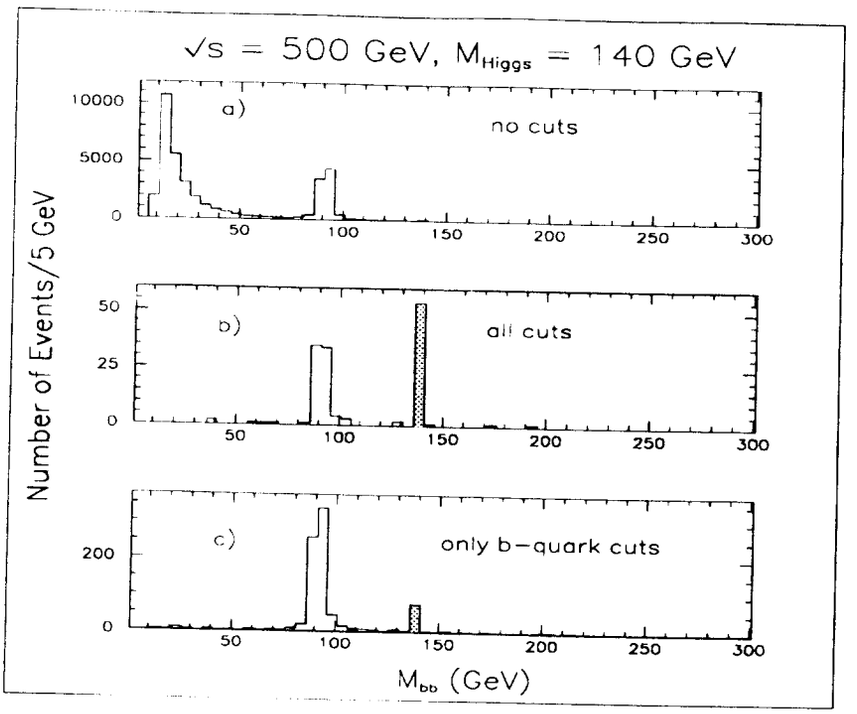

Figure 8: Number of events of the reaction $e^+e^- \to e^+e^- \, b\bar{b}$ as function of the $b\bar{b}$ invariant mass at 500 GeV for an integrated luminosity of 10 fb^{-1}.

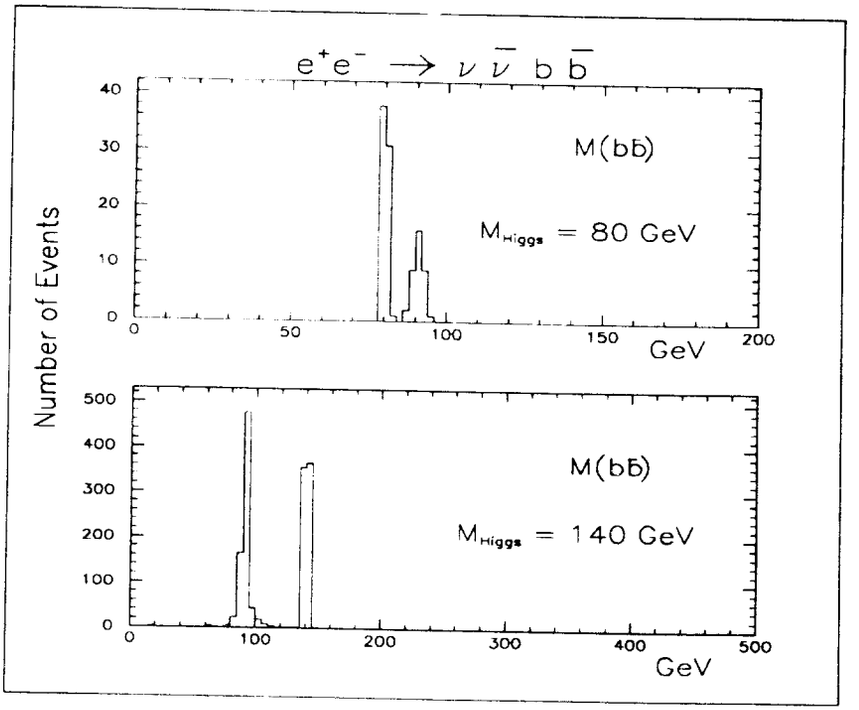

Figure 9: Number of events of the reaction $e^+e^- \to \nu\bar{\nu} \, b\bar{b}$ as function of the $b\bar{b}$ invariant mass at 200 GeV and 500 GeV for an integrated luminosity of 500 pb^{-1} and 10 fb^{-1}, respectively.

The Higgs signal extraction in the $b\bar{b}$ + 2 jet events relies on the total ($b\bar{b}$) energy, the rapidity and the event sphericity [13] even in cases when 4-jet events and some b-tagging inefficiency may fake 4-jet events with two b-jets involved.

5 Summary and conclusions

The results obtained can be summarized as follows.

- For the reactions $e^+e^- \to b\bar{b}$ + 2 fermions the dominant contributions come from the incoherent sum of the 2-to-4 subsets of diagrams, which are based on 2-to-2 and 2-to-3 gauge invariant subreactions.
- Interferences within a given subset of diagrams are important and strong gauge cancellations take place. Interferences between diagrams of different subsets are very small and can be often neglected in realistic simulations. This property allows to build efficient Monte-Carlo generators which imply only the dominating contributions.
- In no case there is a significant impact on the Higgs signal from background diagrams. Interference between Higgsstrahlung and fusion mechanisms of Higgs production is very small as long as $\sqrt{s} > M_Z + M_H$. It is however important below this threshold where Higgs production is small.
- It is important to keep non-zero fermion masses and a correct 2-to-4 body kinematics for precise total rate calculations.
- Cuts on $b\bar{b}$ pair variables like $p_\perp^{b\bar{b}}$, $E_{b\bar{b}}$, and on single $b/\bar{b}$ quantities like $|\cos\Theta_b|$ are very efficient to reduce background while retaining most of the Higgs signal events.

Acknowledgements

We would like to thank V. A. Ilyin and A. E. Pukhov for many discussions and the help with CompHEP calculations. E.B. and S. Sh. would like to thank P. Söding for his interest and support and are grateful to DESY-IfH Zeuthen for the kind hospitality. The work has partially been supported by the ISF grant No. M9B000 and and No. M9B300 and by the INTAS grant INTAS-93-1180. E.B. gratefully acknowledge KEK Minami Tateya group for the financial support during the Morioka conference.

References

[1] S. L. Glashow, Nucl. Phys. **22** (1961) 579;
S. Weinberg, Phys. Rev. Lett. **19** (1967) 1264;
A. Salam, Element. Part. Theory, ed. by N. Svartholm, Stockholm (1968),p. 367.

[2] F. Richard, preprint LAL 94-50 (September 1994).

[3] J. Ellis, M.K. Gaillard, D.V. Nanopoulos, Nucl. Phys. **B106** (1976) 292;
J.D. Bjorken, Proc. of Summer Inst. on Part. Phys., SLAC Report 198(1976).

[4] D.R.T. Jones, S.T. Petkov, Phys. Lett. **B84** (1979) 440;
R.N. Cahn, S. Dawson Phys. Lett. **B136** (1984) 196.

[5] J. F. Gunion, H. E. Haber, G. Kane, S. Dawson, The Higgs Hunter's Guide, Addison-Wesley 1990;
S. Komamiya, Physics and Experiments with Linear Colliders, ed. by R. Orava, P. Eerola, M. Nordberg, World Scientific Publishing Co.,1992,p. 277;
H. E. Haber, ibid. p. 235;
A. Djouadi, D. Haidt, B. A. Kniehl, B. Mele, P. M. Zerwas, Proc. Hamburg, 1991, ed. by P. M. Zerwas, DESY Report 92-123A, p. 11;
P. Janot, preprint LAL 93-38 (July 1993).

[6] V. Barger, K. Cheung, A. Djouadi, B. Kniehl, P. Zerwas, Phys. Rev. **D49** (1994) 79.

[7] E. Boos, M. Sachwitz, H.J. Schreiber, S. Shichanin, Z. Phys. **C61** (1994) 675.

[8] D. Bardin, A. Leike, T. Riemann, Phys. Lett. **B344** (1995) 383;
D. Bardin, A. Leike, T. Riemann, Phys Lett. **B357** (1995) 456.

[9] E. Boos, M. Sachwitz, H.J. Schreiber, S. Shichanin, Int. J. Mod. Phys. **A10** 2067 (1995).

[10] M. Dubinin, V. Edneral, Y. Kurihara, Y. Shimizu, Phys. Lett. **B329** (1994) 379.

[11] E. Boos, M. Sachwitz, H.J. Schreiber, S. Shichanin, Z. Phys. **C64** (1994) 391.

[12] A. Ballestrero, E. Maina, S. Moretti, Nucl. Phys. **B415** (1994) 265;
F.A. Berends, R. Pittau, R. Kleiss, Nucl. Phys. **B424** (1994) 308;

D. Bardin, M. Bilenky, D. Lehner, A. Olchevski, T. Riemann, Nucl. Phys. B(Proc.Suppl.)B37 (1994) 148;
R. Pittau, Phys. Lett. **B335** (1994) 490.

[13] E. Boos, M. Sachwitz, H.J. Schreiber, S. Shichanin, Z. Phys. **C67** (1995) 613.

[14] E. E. Boos et al. Preprint SNVTP-94-116, 1994, 22pp; hep-ph/9503280.

[15] S. Kawabata, Comp. Phys. Commun. **41** (1986) 127.